Atmospheric
Measurement
Techniques
Discussions

Facility for generation of ambient-like model aerosols in the laboratory: application in the intercomparison of automated PM monitors with the reference gravimetric method

Stefan Horender[1], Kevin Auderset[1], Paul Quincey[2], Stefan Seeger[3], Søren Nielsen Skov[4], Kai Dirscherl[5], Thomas O. M. Smith[2], Katie Williams[2], Camille C. Aegerter[1], Daniel M. Kalbermatter[1], François Gaie-Levrel[6] and Konstantina Vasilatou[1]

[1]Federal Institute of Metrology METAS, Bern-Wabern, 3003, Switzerland
[2]National Physical Laboratory (NPL), Teddington, London, UK
[3]Bundesanstalt für Materialforschung und -prüfung (BAM), Berlin, Germany
[4]Bioengineering and Environmental Technology, Danish Technological Institute (DTI), Aarhus, Denmark
[5]Danish National Metrology Institute (DFM), Kogle Alle 5, 2970 Hørsholm, Denmark
[6]Laboratoire national de métrologie et d'essais (LNE), Paris, France

Correspondence to: Konstantina Vasilatou (konstantina.vasilatou@metas.ch)

Abstract. A new facility has been developed which allows for a stable and reproducible generation of ambient-like aerosols in the laboratory. The setup consists of multiple aerosol generators, a custom-made flow tube homogeniser, isokinetic sampling probes and a system to control aerosol temperature and humidity. Model aerosols containing elemental carbon, secondary organic matter from the photo-oxidation of α-pinene, inorganic salts such as ammonium sulphate and ammonium nitrate, mineral dust particles and water were generated at different environmental conditions and different number and mass concentrations. The aerosol physical and chemical properties were characterised with an array of experimental methods, including scanning mobility particle sizing, ion chromatography, total reflection X-ray fluorescence spectroscopy, and thermo-optical analysis. The facility is very versatile and can find applications in the calibration and performance characterisation of aerosol instruments monitoring ambient air. In this study, we performed, as proof of concept, an intercomparison of three different commercial PM (particulate matter) monitors (TEOM 1405, DustTrak DRX 8533 and Fidas Frog) with the gravimetric reference method under three simulated environmental scenarios. The results are presented and compared to previous field studies. We believe that the laboratory-based method for simulating ambient aerosols presented here could provide in the future a useful alternative to time-consuming and expensive field campaigns, which are often required for instrument certification and calibration.

1 Introduction

Atmospheric pollution by airborne particles significantly contributes to climate change and has been linked to respiratory and cardiovascular diseases and lung cancer (Fuzzi et al., 2015; Kim et al., 2015; WHO, 2013). It has been estimated that in Europe alone more than 500,000 deaths per year can be attributed to PM exposure, and that pollution hot spots of PM are responsible for a loss in life expectancy of up to 36 months (Fuzzi et al., 2015). For

Atmospheric
Measurement
Techniques
Discussions

35   EU member states, air quality monitoring - as laid down in the Air Quality Directive 2008/50/EC (European

36   Parliament, 2008, 2015) – is mandatory and comprises quantification of airborne particulate matter and some of its

37   constituents. The most important metric to monitor particulate air pollution is the mass concentration, or more

38   specifically the total mass per unit volume of air of particulate matter which is small enough to pass through a size-

39   selective inlet with a 50 % efficiency cut-off at 2.5 μm or 10 μm aerodynamic diameter, commonly referred to as

40    $PM_{2.5}$ and PM_{10} respectively. Ambient limit values for $PM_{2.5}$ and PM_{10} have been established in Europe (European

41   Parliament, 2008, 2015; FOEN, 2018), the USA (US-EPA, 2016) and other countries worldwide.

42   Regulatory bodies, air quality networks and atmospheric instrument manufacturers all strive to improve air quality

43   monitoring, yet there is still a lack of metrological traceability in airborne PM measurements. PM mass

44   concentration was established as the default metric of PM based on the assumption that mass measurements are

45   straightforward; they can be performed with a conventional balance. The gravimetric filter-based reference methods

46   for PM_{10} and $PM_{2.5}$ are set out in the standards EN 12341:2014 (CEN/TC 264/WG-15, 2014) and EN 14907:2005,

47   however, they fall short in areas such as time resolution and ongoing Quality Assurance and Quality Control to

48   control the effects of semi-volatile particles and water absorption by particles, for example (CEN/TC 264/WG-15,

49   2014; Eisner and Wiener, 2002; Hauck et al., 2004; Zhu et al., 2007). The measurement uncertainties for PM mass

50   concentration in the Directive (European Parliament, 2008, 2015), 25%, are much higher than those for gaseous

51   pollutants (typically 15%).

52   Automatic PM monitoring systems were developed in order to avoid these drawbacks and enable time resolutions

53   below 24 h (Schwab et al., 2006; Weingartner et al., 2011; Zhu et al., 2007); however, demonstrating their

54   equivalence to the reference manual gravimetric method is time consuming and expensive (Hauck et al., 2004; Zhu

55   et al., 2007). There are also inconsistencies in the automatic instruments based on different working principles (e.g.

56   light scattering, beta absorption, oscillating microbalance) and the variations of the aerosols used for comparison.

57   Ambient PM is not uniform with respect to chemical composition, particle size and shape. In most cases, PM does

58   not refer to a single pollutant with a distinct chemical signature, but rather to a highly variable mixture of

59   combustion particles, salts, mineral dust, organic substances and other materials (Hueglin et al., 2005; Putaud et al.,

60   2010). Therefore, suitable standard calibration aerosols do not currently exist.

61   To date, automated PM instruments which are used for regulatory purposes (e.g. at national air quality monitoring

62   stations) are tested for equivalence with the manual gravimetric reference method in monitoring sites using real

63   ambient air (EC-WG, 2010; Hauck et al., 2004). This requires long and expensive testing campaigns at multiple sites

64   during different times of the year in an attempt to include all representative meteorological conditions and the

65   temporal and spatial variations of the ambient air composition. Portable and cost-effective PM monitors, such as the

66   DustTrak (TSI Inc., USA) and Fidas Frog (Palas, Hermany), which are mostly employed for industrial/occupational

67   hygiene surveys (Asbach et al., 2018; Davison et al., 2019; Grzyb and Lenart-Boron, 2019), outdoor (Kingham et

68   al., 2006; Viana et al., 2015; Wallace et al., 2011) and indoor (Chowdhury et al., 2013; Manibusan and Mainelis,

69   2020; Zhou et al., 2016) air quality investigations, process or emissions monitoring (Al-Attabi et al., 2017; Crilley et

70   al., 2012; Grall et al., 2018; McNamara et al., 2011) and aerosol research studies, do not necessarily go through

71   equivalence testing. Instead, they are often calibrated in the laboratory with simple model aerosols, e.g. with dust or

72 salt particles (Hogrefe et al., 2004; Liu et al., 2017; Papapostolou et al., 2017; Schwab et al., 2004) or dried organic

73 particles, such as sucrose and adipic acid (Zhang et al., 2018). Such model aerosols, however, are only partially

74 representative of ambient air since they fail to account for carbonaceous particles and the complex organic matter,

75 which constitute a considerable mass fraction of airborne particulates (Hueglin et al., 2005; Putaud et al., 2010).

76 Light-scattering PM monitors are very sensitive to the aerosol size distribution, refractive index (i.e. chemistry) and

77 humidity, and research findings suggest that a rigorous calibration with "tailored" aerosols, i.e. aerosols

78 representative of the environment of their intended use, is needed (Jayaratne et al., 2020; McNamara et al., 2011).

79 The goal of this study was to develop a standardised laboratory-based calibration procedure for automatic

80 PM-measuring instruments under well-controlled and reproducible experimental conditions. Multi-component

81 model aerosols were generated in order to reproduce the main properties of real ambient air in terms of particle size

82 distribution, chemical composition and number/mass concentration, including semi-volatility and hygroscopicity.

83 The properties of ambient air, of course, may differ dramatically from place to place. Here, the main focus was on

84 simulating aerosols encountered in Europe (Putaud et al., 2010), which are dominated by organic matter, inorganic

85 ions (predominantly sulphate and nitrate, and to a lesser extent ammonium), carbonaceous particles (mostly from

86 fossil fuel combustion rather than biomass burning), mineral dust and water.

87 Apart from the aerosol generation system, the new setup comprises a flow tube homogeniser and a system for

88 reference gravimetric measurements. The facility is very versatile: the total PM mass concentration of the model

89 aerosols can be adjusted in a range from a few $\mu g/m^3$ up to about 500 $\mu g/m^3$, the % fraction of each PM constituent

90 can be tuned to simulate different urban, suburban or rural aerosols and the aerosol temperature and relative

91 humidity can be adjusted to simulate winter or summer-like environmental conditions. As a proof of concept, three

92 different automated PM monitors, the TEOM 1405 (Thermo Scientific, USA), the DustTrak DRX 8533 (TSI Inc.,

93 USA) and the Fidas Frog (Palas, Germany), were compared with the reference gravimetric method under three

94 different environmental scenarios. To our knowledge, this is the very first intercomparison involving the Fidas Frog.

95 Here, we focused on the calibration of the PM monitors' particle quantification, rather than the particle inlet size-

96 selection; i.e. the TEOM 1405 unit was calibrated without its PM sampling inlet. The Fidas Frog and DustTrak DRX

97 8533, which are optical instruments, do not possess any size-selective inlet. The facility could be, however, extended

98 in the future to calibrate PM monitors together with their sampling inlets, if needed. Finally, the facility for

99 generating ambient-like model aerosols presented in this study is not only relevant for the calibration of PM

100 monitors but can find applications in the performance evaluation and quality assurance of other aerosol instruments

101 meant for monitoring ambient, indoor and workplace air as well as in controlled health studies and in vitro

102 toxicology.

103 **2 Design and validation of the experimental setup**

104 The experimental setup consists of three distinct parts: i) the generators of the primary aerosols (dust, salts, soot and

105 aged soot), ii) a flow tube homogeniser for aerosol mixing, including isokinetic sampling probes and ii) a system for

106 reference gravimetric measurements. Each part is described in more detail in the following subsections.

Atmospheric
Measurement
Techniques
Discussions

2.1 Aerosol generation

Four primary aerosols, fresh soot, aged (i.e. organically coated) soot, inorganic salt and mineral dust particles, were generated as depicted in Fig. 1. Fresh soot particles were generated with a miniCAST 6204 burner (Jing Ltd., Switzerland). The operation point was optimised to produce combustion particles with a geometric mean mobility diameter (GMD) of 90 nm and EC/TC (elemental carbon to total carbon) mass fraction of >90 %. The combustion aerosol was split in two portions; one portion was led to the exhaust and the other through a metallic agglomeration tube (1.2 m long, 5 mm internal diameter), where the soot particles grew to about 120 nm. The combustion aerosol was subsequently diluted by a factor of 10 with a VKL10 dilution unit (Palas, Germany). The outlet flow was delivered into an oxidation flow reactor known as Micro Smog Chamber (MSC prototype (Bruns et al., 2015; Corbin et al., 2015b, 2015a; Keller and Burtscher, 2012), developed by A. Keller et al. (Keller and Burtscher, 2012)), where soot was mixed with a controlled amount of α-pinene vapours (≥97 % purity, Sigma Aldrich, Switzerland) under dry conditions (RH<5 %, measured with a digital humidity sensor FHAD 46 series/Almemo D6, Ahlborn, Germany). The aerosol flow through the MSC was set to 1.2 L/min with the use of a miniature radial air blower (model H015X-525A9 with controller, Micronel AG, Switzerland). α-pinene underwent ozonolysis in the MSC, forming secondary organic aerosol (SOA), part of which condensed on the surface of the soot particles, simulating atmospheric ageing procedures (Ess et al., 2020).

The GMD of the soot mobility size distribution was shifted to 160 nm upon coating with SOA and the EC/TC mass fraction dropped to about 20 %. In parallel, fresh soot particles (120 nm mobility diameter) were sampled from the exhaust of the VKL10 dilution unit with the use of a second Micronel blower at flows between 1 and 2 L/min.

Mineral dust particles (ISO 12103-1 A2 fine test dust, Powder Technology Inc., USA) were generated with a rotating brush generator (RBG 1000, Palas, Germany) and were injected horizontally into an empty vessel, which acted as a swirl separator, filtering out the largest size fraction above PM_{10}. Alternatively, whenever calibration with respect to the $PM_{2.5}$ faction is desired, a $PM_{2.5}$ impactor can be installed right before injecting the dust particles into the homogeniser.

Inorganic salt particles were generated by nebulising aqueous mixtures of ammonium sulphate and ammonium nitrate at various ratios with the use of a TSI 3076 atomiser (TSI Inc., USA). The particles were passed through a 1.5-m-long, spiral-shaped agglomeration tube to increase the GMD of the (number-based) mobility size distribution to about 100 nm (the mass-based aerodynamic size distribution shows a maximum at ≈200 nm). The aim was to simulate the presence of ammonium, nitrate and sulphate ions in the fine mode of atmospheric particle size distributions (Liu et al., 2000; Wall et al., 1988; Zhuang et al., 1999). Although generation of coarse mode nitrate, formed at coastal areas by the reaction of gas-phase nitric acid with sea-salt or soil dust particles, or coarse mode sulphate was not actively pursued, there is evidence (see Sect. 3) of coarse sulphate formation. Presumably, this is either due to internal mixing of sulphate ions and mineral dust particles in the flow tube homogeniser or to deposition of salt particles in the aerosol pipes and consequent re-entrainment of agglomerates, which are larger than the particles initially produced by the generator.

The primary aerosols were introduced into a flow tube homogeniser (see Sect. 2.2) through separate injection ports. The flow of each primary aerosol entering the homogeniser could be regulated with separate mass flow controllers

Atmospheric
Measurement
Techniques
Discussions

144   (Red-y MFC, Vögtlin, Switzerland) by splitting and directing part of the main primary aerosol flow to the exhaust.

145   A filter (HEPA capsule, Pall Corporation, USA) was placed upstream of each MFC to remove the particles from the

146   air flow. All four MFCs were connected to the same aerosol pump (VTE8, Thomas, Germany) as shown in Fig. 1.

147   The mobility diameter and number concentration of the soot and salt particles were determined with a scanning

148   mobility particle sizer (SMPS 4.500, Grimm Aerosol Technik GmbH & Co. KG, Germany, L-DMA, Am-241

149   neutralizer, scan time 695 s). The mass concentration of each primary aerosol was measured with a tapered element

150   oscillating microbalance (TEOM 1405, Thermo Scientific, USA), operated at a flow rate of 3 L/min and a

151   temperature of 30 °C. The TEOM data were recorded via a custom-made LabVIEW routine every 6 s without

152   averaging. The size distribution of the dust particles was measured with a Fidas Frog fine-dust monitor (Palas,

153   Germany) and a high-resolution optical particle counter LAS-X II (Particle Measuring Systems, USA).

154   **2.2 Aerosol homogenisation and sampling**

155   The homogenizer is a 2.3-m-long custom-made stainless steel tube with an inner diameter of 16.4 cm, placed

156   vertically. The design is based on a previous study, but has been significantly improved and the facility has been

157   shortened (Horender et al., 2019). The tube is equipped with five identical inlets, placed at the very top as shown in

158   Fig. 1 and 2(a). Dilution air (filtered, humidity and temperature controlled) is delivered to each one of the inlets at a

159   flowrate of 24 L/min. The air is conditioned in two steps (Niedermeier et al., 2020) in such a way that the

160   humidified air is particle free: First, the dew point is adjusted by passing the air through a Nafion humidifier (Series

161   FC125-240-10MP, PermaPure, USA) filled with water (ultra-analytic grade, Purelab ultra, ELGA, Switzerland) at a

162   preselected water temperature, adjusted between 3 °C and 30 °C with a cryostat/thermostat (LAUDA Ecoline

163   Staredition RE 306, Lauda DR. R. Wobser GmbH & Co. KG, Germany). After the Nafion humidifier, the air is fully

164   saturated with water. Subsequently, the air is guided through a heated hose (Series T-7000, Thermocoax Isopad

165   GmbH, Germany), where the temperature can be adjusted up to 100 °C. The temperature and RH of the aerosol were

166   monitored in the homogeniser at the height of the sampling probes with digital sensors (FHAD 46 series/Almemo

167   D6, Ahlborn, Germany).

168   The primary aerosols are injected in the middle of the tube through separate ports located 50 cm downstream as

169   shown in Fig. 2(b). The dilution air sweeps the particles down the tube, where they are further mixed by three

170   turbulent jets of air. The three air-jet injection tubes (flow rate 20 L/min each) are placed symmetrically around the

171   homogenizer tube pointing 60° downwards (Fig. 2(b)). The total flow rate of the homogenised aerosol is hence

172   equal to 180 L/min plus the flows of the four primary aerosols (in total less than 10 L/min). The temperature and

173   relative humidity of the air-jets are adjusted as described above for the dilution air. Finally, the homogeniser is

174   surrounded by copper tubes with flowing water in order to maintain the stainless-steel tube at the same temperature

175   as the aerosol. The temperature of water is adjusted by a flow-type cooler (AS-160 Green Line, Lindr, Czech

176   Republic) or a thermostat (LAUDA EcoGold E4, Lauda DR. R. Wobser GmbH & Co. KG, Germany). The water

177   flows in a closed loop, i.e. circulates back to the cryo/thermostat as shown in Fig. 1. Currently, the homogeniser can

178   only be cooled down to about 10 °C, and this poses limitations to the environmental conditions which can be

Atmospheric
Measurement
Techniques
Discussions

179   simulated in the laboratory; even though the aerosol entering the homogeniser can be preconditioned at a

180   temperature down to about 5 °C, the aerosol temperature at the outlet of the homogeniser will always be ≥10 °C.

181   The sampling zone is located 1.25 m downstream of the injection position and accommodates isokinetic sampling

182   probes (funnels) placed at the bottom end of the homogenizer as illustrated in Fig. 2(c). Isokinetic conditions are

183   necessary when sampling with instruments operating at different flow rates to ensure representative sampling, e.g.

184   by minimizing sampling artefacts of larger particles. Several custom-made sampling probes with different cross

185   sections have been therefore designed to match the flow rate of the various automated PM monitors, which typically

186   ranges between 0.2 L/min and 20 L/min. It is worth noting that the sampling system is highly adaptable; the lower

187   end (outlet) of each sampling probe has custom-made threads so that it can be screwed in and out of the bottom

188   metallic plate of the homogeniser. This ensures that the sampling probes can be readily exchanged before each

189   experiment depending on the specifications of the PM monitors under test. Finally, the excess aerosol flow exits the

190   homogeniser through an exhaust outlet connected to a vacuum line as illustrated schematically in Fig. 1.

191   To characterise the aerosol homogeneity in the flow tube as a function of particle size, sodium chloride (NaCl)

192   particles with a geometric mean mobility diameter of 50 nm and mineral dust particles with aerodynamic diameter in

193   the lower μm range (ISO A2 dust) were generated with a nebuliser and a rotating-brush generator, respectively, as

194   described in Sect. 2.1. Two parallel sampling lines were inserted into the flow tube at the height where the sampling

195   probes would be normally located; the position of the first sampling line was kept fixed at the centre of the flow tube

196   (radial position 0) whereas the second one was placed consecutively at a distance i = -70 mm, -50 mm, -30 mm, -10

197   mm, + 10 mm, + 30 mm, +50 mm and +70 mm with respect to the centre. The outlet of each sampling line was

198   connected to a calibrated CPC (Models 3775 and 3776, respectively, TSI inc., USA). In total, concentration

199   measurements at eight different positions along the diameter of the flow tube were performed. The particle number

200   concentration measured at the centre was used as reference (C_{ref} = C_0) and the aerosol homogeneity was calculated

201   as C_i/C_{ref}. The flow rate of each CPC was 0.3 L/min and the inner diameter of the sampling line was 6 mm. This

202   configuration ensured nearly isokinetic sampling.

203   The tests were performed with NaCl and mineral dust particles separately. In both cases the aerosol spatial

204   homogeneity was found to be well within 3 % in number concentration as shown in Fig. 3(a) and (b), respectively,

205   indicating that the particle mixing characteristics do not depend on particle size in the tested range (i.e. from lower

206   nm to lower μm range). A final test was performed by mixing NaCl and dust particles to investigate whether the

207   particle mixing properties are affected when two primary aerosols are introduced into the homogeniser

208   simultaneously. It was confirmed that the aerosol homogeneity remains well within ±3 % (measurements not

209   shown), indicating that the simultaneous injection of primary aerosols into the homogeniser through separate ports

210   (see Fig. 2(b)) does not compromise particle mixing in any way.

211   By calculating the standard deviation of all 28 measured data points, the spatial inhomogeneity of the aerosol in

212   terms of number concentration was found to be 1.3 % for coverage factor k=1 or 2.6 % for k=2. This is used as an

213   estimate for the uncertainty of the aerosol spatial homogeneity η_{hom} (see 4th row of Table 1). This is a crucial

214   parameter which had not been evaluated so rigorously, if at all, in previous chamber studies (Hogrefe et al., 2004;

215   Liu et al., 2017; Papapostolou et al., 2017; Schwab et al., 2004; Zhu et al., 2007).

2.3 Reference gravimetric method

216

217 The reference method used in this study for determining the PM_{10} or $PM_{2.5}$ mass concentrations of particulate matter
218 in the synthetic ambient aerosols is similar to the method described in the standard EN 12341:2014 (CEN/TC
219 264/WG-15, 2014), i.e. particulate matter was sampled on filters and weighed by means of a balance. The only
220 major deviation from the requirements of the standard is the absence of any size-selective inlets upstream of the
221 automatic PM samplers and the filter holder of the reference gravimetric method.

222 Briefly, model aerosols were drawn through 47 mm PTFE-coated glass fibre filters (Measurement Technology
223 Laboratories, USA) placed in a metallic filter holder (C806 standard aerosol filter holder, Merck Millipore,
224 Germany). The aerosol flow was controlled with a needle valve and measured with a calibrated mass flow meter
225 (Natec Sensors GmbH, Germany) connected to an aerosol pump (VTE8, Thomas, Germany) in such a way that the
226 volumetric flow corresponded to 2.3 m³/h at ambient conditions. Here, ambient condition refers to the aerosol
227 temperature and pressure in the homogeniser at the height of the sampling probes. In the EN 12341 standard, the
228 requirement that the aerosol flow be set to 2.3 m³/h (=38.33 L/min) at ambient conditions arises from the need to
229 accurately define the size cut-off of the PM inlets, a property that depends on the inlet flow. Since the custom-made
230 facility developed in this study aims at calibrating the PM monitors without their respective PM inlet, this flow
231 requirement is here largely superfluous, apart from effects on sampling from the velocity of air through the filter.
232 Nevertheless, during the experiments the aerosol flow was set to 2.3 m³/h at ambient conditions to facilitate
233 comparison between the conventional field-based and the new laboratory-based procedures. The connecting tube
234 between the isokinetic sampling probe (i.e. central sampling funnel in Fig. 2(c)) and the filter holder was made of
235 inert, electrically conducting rubber material and was kept as short as possible (≈ 5 cm) without bends to minimize
236 deposition losses of particulate matter by kinetic processes as well as losses due to thermal, chemical or electrostatic
237 processes. Finally, the laboratory temperature and pressure were kept constant at (21 ± 1) °C and (950 ± 20) hPa,
238 respectively.

239 Before sampling, the filters were conditioned and weighed at NPL and shipped in individual plastic containers to
240 METAS. After sampling, the filter samples were placed in Petri dishes, wrapped tightly in plastic cover and stored at
241 4 °C for about a week. They were then shipped to NPL for conditioning and weighing. NPL use a Measurement
242 Technology Laboratories robotic filter weighing system that comprises an environmental chamber (20 °C ± 1 °C and
243 47.5 % ± 2.5 % relative humidity), an autohandler system and a Mettler Toledo XP2U balance. The filters are
244 conditioned in the chamber for 48 hours before weighing. The filters are weighed, then the system pauses for 24
245 hours before reweighing the filters to identify any time-variation in filter mass. Numerous QA/QC checks are made
246 before each set of weighings.

2.4 Uncertainty budget for the laboratory-based calibration of PM monitors

247

248 The reference mass concentration, $C_{m,ref}$, is given by the equation $C_{m,ref} = \eta_{hom} \frac{m}{V} P_{rel}$, where η_{hom} is the aerosol
249 homogeneity in the flow tube, m is the particulate mass collected on the filter and V is the sampled volume. V is
250 given by the aerosol flow through the filter, Q, multiplied by the time duration of the measurement t. P_{rel} is defined

251   as the relative particle penetration, $P_{rel} = P_{DUT}/P_{ref}$, where P_{DUT} and P_{ref} is the penetration through the sampling

252   probe and connecting tube of the device under test (DUT) and the reference method, respectively. The associated

253   uncertainties are listed in Table 1.

254   Since sampling is carried out with isokinetic sampling probes and the tubes leading to the filter holder and the DUT

255   are kept straight and as short as possible, particle losses are minimised. Penetration P_{rel} was set to 1, however, an

256   uncertainty of 2 % was assigned to account for the higher impaction losses of supermicrometre particles in the

257   sampling funnel of the reference method due to the higher sampling flow (von der Weiden et al., 2009). These losses

258   are to some extent counteracted by the lower diffusion losses of submicrometre particles, which decrease with

259   increasing sampling flow. Here, we followed a rather conservative approach and kept the uncertainty of P_{rel} at 2 %.

260   ## 3 Chemical characterisation of model aerosols

261   Ion chromatography was performed with a Thermo Scientific Dionex™ ICS-1500 Ion Chromatography System for

262   analysis of Anions and the ICS-2100 model for Cations. The systems consist of a liquid eluent, a high-pressure

263   pump, an automatic sample injector, a guard and separator column, an electrolytic suppressor, and a conductivity

264   cell. Before running a sample, the systems were calibrated using a traceable set of calibration standard solutions,

265   which were prepared in-house. The data produced by the range of calibration standard solutions was used to

266   calculate calibration coefficients, which were used to quantitate the sample ions.

267   Thermo-optical analysis of carbonaceous particles was performed with an OC/EC Analyzer (Lab OC-EC Aerosol

268   Analyzer, Sunset Laboratory Inc., USA), which classified the carbonaceous material as elemental carbon (EC) and

269   organic carbon (OC). The particles were sampled on quartz fiber filters (Advantec, Tokyo, Japan, QR-100, 47 mm).

270   For the analysis, the EUSAAR2-protocol (Cavalli et al., 2010) was modified by extending the last temperature step

271   (850 °C) from 80 s in the original protocol to 120 s in order to ensure complete evolution of carbon (Ess and

272   Vasilatou, 2019). The charring correction for pyrolyzed OC was performed by transmittance. OC, EC and TC (total

273   carbon = sum of OC and EC) masses were calculated by the software based on instrument calibration with sucrose

274   solutions.

275   The elemental composition of the model aerosols was characterised by combining a cascade impactor for PM

276   sampling with Total Reflection X-ray Fluorescence Spectroscopy (TXRF, Bruker TStar S4™, Germany) (Osán et

277   al., 2020). A 13 stage low pressure cascade impactor (Dekati DLPI 10™, Finland) with particle size range from 30

278   nm to 10 µm was modified to sample at a rate of 10 L/min on smooth and clean commercial-grade acrylic discs with

279   30 mm diameter, suitable for TXRF. In TXRF, the incident X-ray beam hits the disc's surface at the total reflection

280   angle. The fluorescence spectrum is detected perpendicular to the surface and is dominated by the contributions

281   from the deposit, i.e. the sampled particles. This allows for the detection of element masses as low as ≈10 to 100 pg

282   and thus short sampling periods. The measured element quantities, combined with the sampled air volume, provide

283   the particle size-selected element mass concentrations in the aerosol. The discs were prepared with a 50 ng Yttrium

284   standard for TXRF calibration.

Atmospheric
Measurement
Techniques
Discussions
Open Access
EGU

285   As example, the TXRF analysis of model aerosol 1 is shown in Fig. 4. The analysis revealed that the mineral dust

286   particles contain primarily the elements Si and Al and it was assumed that these are present as oxides SiO_2 and

287   Al_2O_3. The mass-based aerodynamic distribution of the SiO_2 particles exhibits a maximum in the range 1−2 μm

288   while the Al_2O_3 particles are larger (≈7 μm). Sulphur (i.e. in the form of sulphate ions) appears predominantly in the

289   submicrometre range (aerodynamic diameter of 30 nm−1 μm) but a second weaker mode is visible at ≈4−7 μm, thus

290   simulating the aerodynamic size distribution of sulphates in ambient air (Wall et al., 1988; Zhuang et al., 1999)

291   reasonably well. The coarse mode arises most probably from internal mixing of sulphate ions with mineral dust

292   particles. Since nitrates and sulphates were generated with the same method, nitrates are expected to exhibit a

293   similar bimodal size distribution but this could not be experimentally confirmed since nitrogen is difficult to detect

294   with TXRF spectroscopy. Finally, K^+ and Cl^- ions appear in the micrometre range (>2 μm). It is reasonable to expect

295   that Na^+ ions appear also in this size range, however, this could not be investigated by TXRF. By comparing the

296   results of ion chromatography with those of TXRF spectroscopy, there is no evidence of insoluble potassium.

297   The results of the chemical analysis of the model aerosols with ion chromatography, EC/OC analysis and TXRF

298   spectroscopy are summarised in Table 2 and presented graphically in Fig. 5.

4 Intercomparision of automated PM monitors with the reference gravimetric method

300   Three PM monitors, a TEOM 1405 (Thermo Scientific, USA), a DustTrak DRX 8533 (TSI Inc., USA) and a Fidas

301   Frog (Palas, Germany) were used in this study. The 1405 TEOM takes continuous direct mass measurements of

302   particulates using a tapered element oscillating microbalance and is considered to be one of the most well-

303   established automated instruments for monitoring PM mass concentration at air quality monitoring stations. The

304   DustTrak DRX 8533 and the Fidas Frog aerosol monitors are, unlike TEOM, portable and more cost efficient. These

305   do not measure particle mass directly but record instead the particle number concentration and size distribution

306   using optical techniques, from which they calculate the mass concentration using built-in algorithms.

307   The PM monitors were exposed to three different model aerosols, which were generated in the laboratory with the

308   facility described in Sect. 2. All three model aerosols were ambient-like mixtures, i.e. they contained inorganic salts,

309   elemental carbon (soot), secondary organic matter, mineral dust and water. The aerosol composition was analysed

310   with the methods described in Sect. 3. The chemical composition of the model aerosols and the environmental

311   conditions during each experiment are listed in Table 2 and depicted schematically in Fig. 5. It can be seen that the

312   mass fractions of the different chemical constitutents varied in the range ≈30−40 % OM, ≈5−15 % EC, ≈7−15 %

313   nitrate, ≈5−15 % sulphate, ≈2−3 % ammonium, ≈10−20 % mineral dust and ≈10−20 % other materials.

314   The PM_{10} mass concentration range (20−40 μg/m³) is typical for urban and suburban regions across Europe. The

315   chemical composition is representative of European aerosols containing carbonaceous particles from fossil fuel

316   combustion (rather than biomass burning), secondary organic matter, mineral dust particles and inorganic ions such

317   as ammonium, sulphate, nitrate and sodium. The temperature and relative humidity of the aerosols were controlled

318   in the range ≈10−20 °C and 50−70 %, respectively, to simulate different ambient environmental conditions.

319   The results of the comparison between the automated PM monitors and the reference gravimetric method are shown

320   in Fig. 6. For the automated PM monitors, which measure continuously and with high time resolution, each data

321   point corresponds to the arithmetic average over a 30 min measurement period. The reference method delivers only

322   one data point, i.e. the average PM_{10} mass concentration over the whole measurement period, which is illustrated in

323   the graph as a straight solid line and summarised in Table 2. It must be noted that the operating temperature of the

324   TEOM 1405 monitor was set as low as possible, i.e. to 30 °C, to minimise losses due to (semi)volatile material

325   (Meyer et al., 2000). For the DustTrak and Fidas Frog the default factory settings were used.

326   Figure 6(a) presents the results of the TEOM 1405, Fidas Frog and the reference gravimetric method for model

327   aerosol 1. The results of the DustTrak 8533 are not reported because of a technical problem (obstruction of the

328   aerosol inlet) which compromised the measurement accuracy. The TEOM 1405 seems to agree well with the

329   reference method in the beginning but indicates a decrease of about 15 % in mass concentration at the end of the 4 h

330   measurement. Particle number concentration measurements of the primary aerosols before and after the experiment

331   revealed that the number concentration of the fresh soot particles decreased by about 60 % during the measurement

332   period whereas the number concentration of the dust, salt and aged soot particles remained largely constant. The

333   reason was a defect in the valve regulating the flow of the fresh soot particles into the homogeniser. The decrease in

334   the aerosol mass concentration recorded by the TEOM is therefore real and can be attributed predominantly to the

335   decreasing number and mass concentration of the uncoated soot particles. Since the concentration of the model

336   aerosol decreased during measurement, the best way to assess the performance of the TEOM 1405 with respect to

337   the reference method is to calculate the 4-h-average mass concentration. This amounts to 41.6 µg/m^3 (see Table 3),

338   only 3.7 % lower than the reference measurement (43.2 µg/m^3).

339   The fresh soot particles consist mainly of EC and have a geometric mean mobility diameter of about 120 nm, i.e.

340   below the cut-off limit of the Fidas Frog. Indeed, experiments with miniCAST soot showed that the Fidas Frog and

341   DustTrak 8533 failed to detect soot particles of this size. This explains why the Fidas Frog reported a constant mass

342   concentration over the whole measurement period. In Table 3, it can be seen that the Fidas Frog reported an average

343   PM_{10} mass concentration of 38.8 µg/m^3, i.e. -4.4 µg/m^3 with respect to the reference method. This deviation agrees

344   well with the EC mass concentration of 5.0 µg/m^3 (Table 2), as determined with EC/OC analysis. Note that the cut-

345   off curve of optical instruments depends on the refractive index of the particles: the Fidas Frog fails to detect fresh

346   soot particles below ≈200 nm but detects a consederable mass fraction of the coated soot and salt particles despite

347   their small size.

348   The results obtained with model aerosol 2 are displayed in Fig. 6(b). Here, the concentration of the aerosol remained

349   constant throughout the measurement period. The Fidas Frog and TEOM 1405 monitors underestimate the mass

350   concentration by 29 % and 14 %, respectively, compared to the reference method while the DustTrak 8533

351   overestimates the mass concentration by 50 %. The larger deviation between the TEOM 1405 and the reference

352   method compared to model aerosol 1 results from the winter-like environmental conditions; the temperature of

353   model aerosol 2 was set to 12 °C, the relative humidity to 70 % and the nitrate content was relatively high (about

354   15%) as shown in Table 2. Since the aerosol stream sampled by the TEOM 1405 is heated to 30 °C, a fraction of the

355   (semi)volatile components (e.g. nitrate and secondary organic aerosol) evolves into the gas phase and is therefore

356   not collected on the filter. These results are in agreement with previous studies reporting that TEOM monitors set at

357   a lower temperature than the standard configuration (50 °C) still could lose semivolatile materials (Lee et al., 2005),

358   especially in cooler months (Sofowote et al., 2014; Su et al., 2018).

359   The large positive deviation of the DustTrak 8533 by a factor of about 1.5 is not surprising. Previous studies have

360   found that different DustTrak models over-recorded PM values by a factor of 1.2−3 (Chung et al., 2001; Grzyb and

361   Lenart-Boron, 2019; Heal et al., 2000; Kingham et al., 2006; Liu et al., 2017; McNamara et al., 2011; Wallace et al.,

362   2011; Yanosky et al., 2002) depending on the aerosol properties. It has been suggested that the "over-estimation is a

363   simple calibration issue in which differences between the optical properties of the manufacturer's factory calibration

364   PM (Arizona Road Dust) and the PM under study explained the uniform relative errors recorded" (Kingham et al.,

365   2006). The results are nevertheless puzzling. Considering that the device fails completely to detect fresh soot and

366   underestimates the amount of aged soot, we would have rather expected to observe a negative deviation with respect

367   to the reference method. In any case, the large range of the positive systematic bias (factor of 1.2−3) highlights the

368   need for source-specific calibration procedures against a reference method.

369   in the case of Fidas Frog, if the reading of the monitor (21.0 $\mu g/m^3$, Table 3) is corrected for the undetected mass of

370   fresh soot (3.8 $\mu g/m^3$, Table 2), then the Fidas Frog still underestimates the mass concentration by ≈15 % with

371   respect to the reference method.

372   The results obtained in the case of model aerosol 3 are illustrated in Fig. 6(c). With an average PM_{10} mass

373   concentration of 19.2 $\mu g/m^3$, the TEOM 1405 exhibits an excellent agreement with the reference method (19.3

374    $\mu g/m^3$, see Table 2). The DustTrak 8533 overestimates the mass concentration by approx. 33 %, and thus performs

375   slightly better than in the case of model aerosol 2. Fidas Frog underestimates the mass concentration by about 23 %,

376   or ≈15 % after correction for the undetected mass of fresh soot, in agreement with the findings of the experiment

377   with model aerosol 2. As mentioned above, PM monitors based on light scattering, such as the Fidas Frog and the

378   DustTrak, measure particle number concentration and convert this into mass concentration by using a size-

379   dependent particle density function. This function is integrated into the software of the instrument. Deviations may

380   occur if the built-in functions differ substantially from the real density function of the aerosol. More experiments

381   with ambient-like model aerosols under low and high relative humidity would be needed to define a comprehensive

382   set of calibration factors for these instruments.

5 Conclusions

384   In this study, we present the first steps towards the generation of ambient-like aerosols in the laboratory. A custom-

385   made facility for the stable and reproducible generation of such model aerosols was developed, which presents the

386   following advantages:

387   • The model aerosols are complex, consisting of elemental carbon (fresh soot), soot coated with SOA (aged

388   soot), inorganic ions (such as ammonium, sulphate and nitrate) and mineral dust particles

389   • The aerosol mixture can therefore have a controlled amount of semi-volatile and hygroscopic material

390 • The total PM mass concentration of the model aerosols can be adjusted in a range from a few μg/m^3 up to
391 about 500 μg/m^3 and remains stable over several hours

392 • The % fraction of each PM constituent can be tuned to simulate different urban, suburban or rural aerosols

393 • The size distribution (geometric mean and width of accumulation and coarse mode) can be adjusted by
394 tuning the size distribution of the primary aerosols

395 • The aerosol temperature and relative humidity can be adjusted to simulate winter or summer-like
396 environmental conditions (10−40 °C, 5−90 % RH)

397 • A spatial aerosol homogeneity of 2.6 % (k=2) in number concentration can be attained in the mixing
398 chamber, a parameter not evaluated so rigorously, if at all, in previous chamber studies (Hogrefe et al.,
399 2004; Liu et al., 2017; Papapostolou et al., 2017; Schwab et al., 2004; Zhu et al., 2007)

400 • The isokinetic sampling system is highly adaptable and can accommodate instruments with flows up to at
401 least 40 L/min

402 • The design is much more compact compared to other mixing chambers described in the literature (Hogrefe
403 et al., 2004; Horender et al., 2019; Papapostolou et al., 2017; Schwab et al., 2004; Zhu et al., 2007) and can
404 therefore easily fit into a typical laboratory.

405 As a proof of concept, three different automated PM monitors, the TEOM 1405 (Thermo Scientific, USA), the
406 DustTrak DRX 8533 (TSI Inc., USA) and the Fidas Frog (Palas, Germany), were compared with the reference
407 gravimetric method under three different environmental scenarios. The TEOM 1405, operated at 30 °C, agreed very
408 well with the reference gravimetric method in the case of summertime aerosols (21 °C), but showed a negative
409 deviation in PM$_{10}$ mass concentration of ≈15 % when the model aerosol was conditioned at 12 °C due to losses of
410 semi-volatile material. The Fidas Frog underestimated the PM$_{10}$ mass concentration by ≈10−30 % whereas the
411 DustTrak 8533 overestimated the PM$_{10}$ mass concentration by ≈30−50 % depending on the aerosol chemical
412 composition and environmental conditions.

413 Currently, one limitation of the facility is that the model aerosols cannot be conditioned to temperatures lower than
414 10 °C but this could be improved by thermally insulating the homogeniser (e.g. with black nitrile foam insulation).
415 Moreover, the composition of the model aerosols could be further refined by adding more components, such as
416 metallic particles with the use of a spark-discharge generator, bioaerosols e.g. with a Sparging Liquid Aerosol
417 Generator (SLAG, CH Technologies, USA) and particles from biomass burning. This last step could pose challenges
418 since the mass output is usually not very stable over time and the physicochemical properties of the aerosol depend
419 heavily on the combustion material, as well as the stove design.

420 To conclude, the facility presented in this study can be used to generate ambient-like model aerosols for quality
421 assurance testing, intercomparisons of different instruments and performance evaluation/calibration with respect to
422 PM mass concentration. The same facility could also be used for other PM measurements such as number
423 concentration and absorption properties (e.g. related to black carbon). The aerosol facility also provides excellent
424 opportunities for basic aerosol research and aerosol health-related studies.

425

426 **Data availability**

427 All data presented in the paper are available for research purposes on request to the authors of the paper.

428

429 **Author contribution**

430 *METAS*: SH and KV designed, validated and operated the experimental facility, coordinated the intercomparison

431 and prepared the paper with contributions from all other authors; KA designed the isokinetic sampling probes; CCA

432 assisted during the preparation of the intercomparison and DMK performed EC/OC analysis.

433 *BAM*: StS performed TXRF analysis

434 *NPL*: PQ helped design the study, TS weighed the filter samples and KW performed IC analysis

435 *LNE*: FGL advised on aerosol generation

436 *DFM*: KD performed high-resolution measurements with a reference optical particle counter

437 *DTI:* SNS operated the DustTrak DRX during the intercomparison

438

439 **Competing interests**
440 The authors declare that they have no conflict of interest.

441

442 **Acknowledgments**

443 S. Horender, K. Auderset and K. Vasilatou would like to thank their colleagues at the mechanical and electronic

444 workshop (METAS) for valuable technical assistance throughout this study.

445 This work has received funding from the 16ENV07 Aeromet project of the European Union through the European

446 Metrology Programme for Innovation and Research (EMPIR). EMPIR is jointly funded by the EMPIR participating

447 countries within EURAMET and the European Union. METAS was supported by the Swiss State Secretariat for

448 Education, Research and Innovation (SERI) under contract number 17.00112. The opinions expressed and

449 arguments employed herein do not necessarily reflect the official views of the Swiss Government.

450 # References

451 Al-Attabi, R., Dumme, L. F., Kong, L., Schütz, J. A. and Morsi, Y.: High Efficiency Poly(acrylonitrile) Electrospun

452 Nanofiber Membranes for Airborne Nanomaterials Filtration, Adv. Eng. Mater., 20(1), 1700572,

453 doi:10.1002/adem.201700572, 2017.

454 Asbach, C., Hellack, B., Schumacher, S., Bässler, M., Spreitzer, M., Pohl, T., Weber, K., Monz, C., Bieder, S.,

455 Schultze, T. and Todea, A.: Anwendungsmöglichkeiten und Grenzen kostengünstiger Feinstaubsensoren,

456 Gefahrstoffe-Reinhaltung der Luft, 78(6), 242–250, 2018.

457 Bruns, E. A., El Haddad, I., Keller, A., Klein, F., Kumar, N. K., Pieber, S. M., Corbin, J. C., Slowik, J. G., Brune,

458 W. H., Baltensperger, U. and Prévôt, A. S. H.: Inter-comparison of laboratory smog chamber and flow reactor

459 systems on organic aerosol yield and composition, Atmos. Meas. Tech., 8, 2315–2332, doi:10.5194/amt-8-2315-

460 2015, 2015.

461 Cavalli, F., Viana, M., Yttri, K. E., Genberg, J. and Putaud, J.-P.: Toward a standardised thermal-optical protocol for

462 measuring atmospheric organic and elemental carbon: the EUSAAR protocol, Atmos. Meas. Tech., 3, 79–89,
463 doi:10.5194/amt-3-79-2010, 2010.

464 CEN/TC 264/WG-15: European Standard EN 12341: Ambient air - Standard gravimetric measurement method for
465 the determination of the PM10 or PM2,5 mass concentration of suspended particulate matter, 2014.

466 Chowdhury, Z., Campanella, L., Gray, C., Al Masud, A., Marter-Kenyon, J., Pennise, D., Charron, D. and Zuzhang,
467 X.: Measurement and modeling of indoor air pollution in rural households with multiple stove interventions in
468 Yunnan, China, Atmos. Environ., 67, 161–169, doi:10.1016/j.atmosenv.2012.10.041, 2013.

469 Chung, A., Chang, D. P. Y., Kleeman, M. J., Perry, K. D., Cahill, T. A., Dutcher, D., McDougall, E. M. and Stroud,
470 K.: Comparison of Real-Time Instruments Used To Monitor Airborne Particulate Matter, J. Air Waste Manage.
471 Assoc., 51(1), 109–120, doi:10.1080/10473289.2001.10464254, 2001.

472 Corbin, J. C., Lohmann, U., Sierau, B., Keller, A., Burtscher, H. and Mensah, A. A.: Black carbon surface oxidation
473 and organic composition of beech-wood soot aerosols, Atmos. Chem. Phys., 15, 11885–11907, doi:10.5194/acp-15-
474 11885-2015, 2015a.

475 Corbin, J. C., Keller, A., Lohmann, U., Burtscher, H., Sierau, B. and Mensah, A. A.: Organic Emissions from a
476 Wood Stove and a Pellet Stove Before and After Simulated Atmospheric Aging Organic Emissions from a Wood
477 Stove and a Pellet Stove Before and After Simulated Atmospheric Aging, Aerosol Sci. Technol., 49(11), 1037–
478 1050, doi:10.1080/02786826.2015.1079586, 2015b.

479 Crilley, L. R., Knibbs, L. D., Miljevic, B., Cong, X., Fairfull-Smith, K. E., Bottle, S. E., Ristovski, Z. D., Ayoko, G.
480 A. and Morawska, L.: Concentration and oxidative potential of on-road particle emissions and their relationship with
481 traffic composition: Relevance to exposure assessment, Atmos. Environ., 59, 533–539,
482 doi:10.1016/j.atmosenv.2012.05.039, 2012.

483 Davison, J. A., Wylie, C. E., McGladdery, C. E., Fettes, C., Haggett, E. F. and Ramzan, P. H. L.: Airborne
484 particulate size and concentrations in five Thoroughbred training yards in Newmarket (UK), Vet. J., 248, 48–50,
485 doi:10.1016/j.tvjl.2019.04.006, 2019.

486 EC-WG: Guidance to the demonstration of equivalence of ambient air monitoring methods, Report by an EC
487 Working Group on Guidance for the Demonstration of Equivalence, [online] Available from:
488 http://ec.europa.eu/environment/air/quality/legislation/assessment.htm (Accessed 31 August 2020), 2010.

489 Eisner, A. D. and Wiener, R. W.: Discussion and Evaluation of the Volatility Test for Equivalency of Other
490 Methods to the Federal Reference Method for Fine Particulate Matter, Aerosol Sci. Technol., 36(4), 433–440,
491 doi:10.1080/027868202753571250, 2002.

492 El-Zanan, H. S., Lowenthal, D. H., Zielinska, B., Chow, J. C. and Kumar, N.: Determination of the organic aerosol
493 mass to organic carbon ratio in IMPROVE samples, Chemosphere, 60, 485–496,
494 doi:10.1016/j.chemosphere.2005.01.005, 2005.

495 Ess, M. N. and Vasilatou, K.: Characterization of a new miniCAST with diffusion flame and premixed flame
496 options: Generation of particles with high EC content in the size range 30 nm to 200 nm, Aerosol Sci. Technol.,
497 53(1), 29–44, doi:10.1080/02786826.2018.1536818, 2019.

498 Ess, M. N., Berto, M., Keller, A., Gysel, M. and Vasilatou, K.: Laboratory generated coated-soot particles with

Atmospheric
Measurement
Techniques
Discussions

499   tunable, well-controlled properties using a miniCAST BC and a micro smog chamber (to be submitted), 2020.

500   European Parliament: Directive 2008/50/EC of the European Parliament and of the Council of 21 May 2008 on

501   ambient air quality and cleaner air for Europe (OJ L 152, 11.6.2008, p. 1–44), [online] Available from: https://eur-

502   lex.europa.eu/legal-content/en/ALL/?uri=CELEX%3A32008L0050 (Accessed 31 August 2020), 2008.

503   European Parliament: Consolidated text: Directive 2008/50/EC of the European Parliament and of the Council of 21

504   May 2008 on ambient air quality and cleaner air for Europe, [online] Available from: https://eur-lex.europa.eu/legal-

505   content/EN/TXT/?uri=CELEX:02008L0050-20150918 (Accessed 31 August 2020), 2015.

506   FOEN: Fine particles, [online] Available from: https://www.bafu.admin.ch/bafu/en/home/topics/air/info-

507   specialists/air-quality-in-switzerland/fine-particles.html (Accessed 31 August 2020), 2018.

508   Fuzzi, S., Baltensperger, U., Carslaw, K., Decesari, S., Denier Van Der Gon, H., Facchini, M. C., Fowler, D., Koren,

509   I., Langford, B., Lohmann, U., Nemitz, E., Pandis, S., Riipinen, I., Rudich, Y., Schaap, M., Slowik, J. G., Spracklen,

510   D. V, Vignati, E., Wild, M., Williams, M. and Gilardoni, S.: Particulate matter, air quality and climate: lessons

511   learned and future needs, Atmos. Chem. Phys., 15, 8217–8299, doi:10.5194/acp-15-8217-2015, 2015.

512   Grall, S., Debéda, H., Dufour, I. and Aubry, V.: Screen-Printed Microcantilevers for Environmental Sensing,

513   Proceedings, 2, 722, doi:10.3390/proceedings2130722, 2018.

514   Grzyb, J. and Lenart-Boron, A.: Bacterial bioaerosol concentration and size distribution in the selected animal

515   premises in a zoological garden, Aerobiologia (Bologna)., 35, 253–268, doi:10.1007/s10453-018-09557-9, 2019.

516   Hauck, H., Berner, A., Gomiscek, B., Stopper, S., Puxbauma, H., Kundi, M. and Preining, O.: On the equivalence of

517   gravimetric PM data with TEOM and beta-attenuation measurements, J. Aerosol Sci., 35, 1135–1149,

518   doi:10.1016/j.jaerosci.2004.04.004, 2004.

519   Heal, M. R., Beverland, I. J., McCabe, M., Hepburn, W. and Agius, R. M.: Intercomparison of five PM10

520   monitoring devices and the implications for exposure measurement in epidemiological research, J. Environ. Monit.,

521   2, 455–461, doi:10.1039/b002741n, 2000.

522   Hogrefe, O., Drewnick, F., Garland Lala, G., Schwab, J. J. and Demerjian, K. L.: Development, Operation and

523   Applications of an Aerosol Generation, Calibration and Research Facility Special Issue of Aerosol Science and

524   Technology on Findings from the Fine Particulate Matter Supersites Program, Aerosol Sci. Technol., 38, 196–214,

525   doi:10.1080/02786820390229516, 2004.

526   Horender, S., Auderset, K. and Vasilatou, K.: Facility for calibration of optical and condensation particle counters

527   based on a turbulent aerosol mixing tube and a reference optical particle counter, Rev. Sci. Instrum., 90, 075111,

528   doi:10.1063/1.5095853, 2019.

529   Hueglin, C., Gehrig, R., Baltensperger, U., Gysel, M., Monn, C. and Vonmont, H.: Chemical characterisation of

530   PM2.5, PM10 and coarse particles at urban, near-city and rural sites in Switzerland, Atmos. Environ., 39, 637–651,

531   doi:10.1016/j.atmosenv.2004.10.027, 2005.

532   Jayaratne, R., Liu, X., Ahn, K.-H., Asumadu-Sakyi, A., Fisher, G., Gao, J., Mabon, A., Mazaheri, M., Mullins, B.,

533   Nyarku, M., Ristovski, Z., Scorgie, Y., Phong, T., Dunbabin, M. and Morawska, L.: Low-cost PM2.5 Sensors: An

534   Assessment of their Suitability for Various Applications, Aerosol Air Qual. Res., 20, 520–532,

535   doi:10.4209/aaqr.2018.10.0390, 2020.

536   Keller, A. and Burtscher, H.: A continuous photo-oxidation flow reactor for a defined measurement of the SOA
537   formation potential of wood burning emissions, J. Aerosol Sci., 49(12), 9–20, doi:10.1016/j.jaerosci.2012.02.007,
538   2012.

539   Kim, K.-H., Kabir, E. and Kabir, S.: A review on the human health impact of airborne particulate matter, Environ.
540   Int., 74, 136–143, doi:10.1016/j.envint.2014.10.005, 2015.

541   Kingham, S., Durand, M., Aberkane, T., Harrison, J., Wilson, J. G. and Epton, M.: Winter comparison of TEOM,
542   MiniVol and DustTrak PM10 monitors in a woodsmoke environment, Atmos. Environ., 40, 338–347,
543   doi:10.1016/j.atmosenv.2005.09.042, 2006.

544   Lee, J. H., Hopke, P. K., Holsen, T. M. and Polissar, A. V: Evaluation of Continuous and Filter-Based Methods for
545   Measuring PM2.5 Mass Concentration, Aerosol Sci. Technol., 39, 290–303, doi:10.1080/027868290929323, 2005.

546   Liu, D.-Y., Prather, K. A. and Hering, S. V.: Variations in the Size and Chemical Composition of Nitrate-Containing
547   Particles in Riverside, CA, Aerosol Sci. Technol., 33, 71–86, doi:10.1080/027868200410859, 2000.

548   Liu, D., Zhang, Q., Jiang, J. and Chen, D.: Performance calibration of low-cost and portable particular matter (PM)
549   sensors, J. Aerosol Sci., 112(May), 1–10, doi:10.1016/j.jaerosci.2017.05.011, 2017.

550   Manibusan, S. and Mainelis, G.: Performance of Four Consumer-grade Air Pollution Measurement Devices in
551   Different Residences, Aerosol Air Qual. Res., 20, 217–230, doi:10.4209/aaqr.2019.01.0045, 2020.

552   McNamara, M. L., Noonan, C. W. and Ward, T. J.: Correction Factor for Continuous Monitoring of Wood Smoke
553   Fine Particulate Matter, Aerosol Air Qual. Res., 11, 315–322, doi:10.4209/aaqr.2010.08.0072, 2011.

554   Meyer, M. B., Patashnick, H., Ambs, J. L. and Rupprecht, E.: Development of a Sample Equilibration System for
555   the   TEOM   Continuous   PM   Monitor,   J.   Air   Waste   Manage.   Assoc.,   50(8),   1345–1349,
556   doi:10.1080/10473289.2000.10464180, 2000.

557   Niedermeier, D., Voigtländer, J., Schmalfuß, S., Busch, D., Schumacher, J., Shaw, R. A. and Stratmann, F.:
558   Characterization and first results from LACIS-T: a moist-air wind tunnel to study aerosol – cloud – turbulence
559   interactions, Atmos. Meas. Tech., 13, 2015–2033, doi:10.5194/amt-13-2015-2020, 2020.

560   Osán, J., Börcsök, E., Czömpöly, O., Dian, C., Groma, V., Stabile, L. and Török, S.: Experimental evaluation of the
561   in-the-field capabilities of total-reflection X-ray fluorescence analysis to trace fine and ultrafine aerosol particles in
562   populated areas, Spectrochim. Acta Part B, 167, 105852, doi:10.1016/j.sab.2020.105852, 2020.

563   Papapostolou, V., Zhang, H., Feenstra, B. J. and Polidori, A.: Development of an environmental chamber for
564   evaluating the performance of low-cost air quality sensors under controlled conditions, Atmos. Environ., 171, 82–
565   90, doi:10.1016/j.atmosenv.2017.10.003, 2017.

566   Putaud, J.-P., Dingenen, R. Van, Alastuey, A., Bauer, H., Birmili, W., Cyrys, J., Flentje, H., Fuzzi, S., Gehrig, R.,
567   Hansson, H. C., Harrison, R. M., Herrmann, H., Hitzenberger, R., Hüglin, C., Jones, A. M., Kasper-Giebl, A., Kiss,
568   G., Kousa, A., Kuhlbusch, T. A. J., Löschau, G., Maenhaut, W., Molnar, A., Moreno, T., Pekkanen, J., Perrino, C.,
569   Pitz, M., Puxbaum, H., Querol, X., Rodriguez, S., Salma, I., Schwarz, J., Smolik, J., Schneider, J., Spindler, G., ten
570   Brink, H., Tursic, J., Viana, M., Wiedensohler, A. and Raes, F.: A European aerosol phenomenology - 3: Physical
571   and chemical characteristics of particulate matter from 60 rural, urban, and kerbside sites across Europe, Atmos.
572   Environ., 44, 1308–1320, doi:10.1016/j.atmosenv.2009.12.011, 2010.

573 Schwab, J. J., Hogrefe, O., Demerjian, K. L. and Ambs, J. L.: Laboratory Characterization of Modified Tapered
574 Element Oscillating Microbalance Samplers, J. Air Waste Manage. Assoc., 54(10), 1254–1263,
575 doi:10.1080/10473289.2004.10471019, 2004.

576 Schwab, J. J., Felton, H. D., Rattigan, O. V and Demerjian, K. L.: New York State Urban and Rural Measurements
577 of Continuous PM 2.5 Mass by FDMS, TEOM, and BAM, J. Air Waste Manage. Assoc., 56(4), 372–383,
578 doi:10.1080/10473289.2006.10464523, 2006.

579 Sofowote, U., Su, Y., Bitzos, M. M. and Munoz, A.: Improving the correlations of ambient tapered element
580 oscillating microbalance PM2.5 data and SHARP 5030 Federal Equivalent Method in Ontario: A multiple linear
581 regression analysis, J. Air Waste Manage. Assoc., 61(1), 104–114, doi:10.1080/10962247.2013.833145, 2014.

582 Su, Y., Sofowote, U., Debosz, J., White, L. and Munoz, A.: Multi-Year Continuous PM2.5 Measurements with the
583 Federal Equivalent Method SHARP 5030 and Comparisons to Filter-Based and TEOM Measurements in Ontario,
584 Canada, Atmosphere (Basel)., 9, 1–13, doi:10.3390/atmos9050191, 2018.

585 US-EPA: National Ambient Air Quality Standards published by the United States Environment Protection Agency,
586 [online] Available from: https://www.epa.gov/criteria-air-pollutants/naaqs-table (Accessed 31 August 2020), 2016.

587 Viana, M., Rivas, I., Reche, C., Fonseca, A., Perez, N., Querol, X., Alastuey, A., Alvarez-Pedrerol, M. and Sunyer,
588 J.: Field comparison of portable and stationary instruments for outdoor urban air exposure assessments, Atmos.
589 Environ., 123, 220–228, doi:10.1016/j.atmosenv.2015.10.076, 2015.

590 Wall, S. M., Walter, J. and Ondo, J. L.: Measurement of aerosol size distributions for nitrate and major ionic species,
591 Atmos. Environ., 22(8), 1649–1656, doi:10.1016/0004-6981(88)90392-7, 1988.

592 Wallace, L. A., Wheeler, A. J., Kearney, J., Van Ryswyk, K., You, H., Kulka, R. H., Rasmussen, P. E., Brook, J. R.
593 and Xu, X.: Validation of continuous particle monitors for personal, indoor, and outdoor exposures, J. Expo. Sci.
594 Environ. Epidemiol., 21, 49–64, doi:10.1038/jes.2010.15, 2011.

595 von der Weiden, S.-L., Drewnick, F. and Borrmann, S.: Particle Loss Calculator – a new software tool for the
596 assessment of the performance of aerosol inlet systems, Atmos. Meas. Tech., 2, 479–494, doi:10.5194/amt-2-479-
597 2009, 2009.

598 Weingartner, E., Burtscher, H., Hüglin, C. and Ehara, K.: Semi-continuous mass measurement, in Aerosol
599 Measurement: Principles, Techniques, and Applications, edited by P. Kulkarni, P. A. Baron, and K. Willeke, pp.
600 155–168, John Wiley & Sons, Inc., Hoboken, New Jersey., 2011.

601 WHO: Review of evidence on health aspects of air pollution – REVIHAAP Project. [online] Available from:
602 https://www.euro.who.int/en/health-topics/environment-and-health/air-quality/publications/2013/review-of-
603 evidence-on-health-aspects-of-air-pollution-revihaap-project-final-technical-report, 2013.

604 Yanosky, J. D., Williams, P. L. and Macintosh, D. L.: A comparison of two direct-reading aerosol monitors with the
605 federal reference method for PM2.5 in indoor air, Atmos. Environ., 36, 107–113, doi:10.1016/S1352-
606 2310(01)00422-8, 2002.

607 Zhang, J., Marto, J. P. and Schwab, J. J.: Exploring the applicability and limitations of selected optical scattering
608 instruments for PM mass measurement, Atmos. Meas. Tech., 11, 2995–3005, doi:10.5194/amt-11-2995-2018, 2018.

609 Zhou, Z., Liu, Y., Yuan, J., Zuo, J., Chen, G., Xu, L. and Rameezdeen, R.: Indoor PM2.5 concentrations in

610   residential buildings during a severely polluted winter: A case study in Tianjin, China, Renew. Sustain. Energy Rev.,

611   64, 372–381, doi:10.1016/j.rser.2016.06.018, 2016.

612   Zhu, K., Zhang, J. J. and Lioy, P. J.: Evaluation and Comparison of Continuous Fine Particulate Matter Monitors for

613   Measurement of Ambient Aerosols, J. Air Waste Manage. Assoc., 57(12), 1499–1506, doi:10.3155/1047-

614   3289.57.12.1499, 2007.

615   Zhuang, H., Chan, C. K., Fang, M. and Wexler, A. S.: Size distributions of particulate sulfate, nitrate, and

616   ammonium at a coastal site in Hong Kong, Atmos. Environ., 33(6), 843–853, doi:10.1016/S1352-2310(98)00305-7,

617   1999.

618

619

620

621

622

623

624

625

626

627

628

629

630

631

632

633

634

635

636

637

638

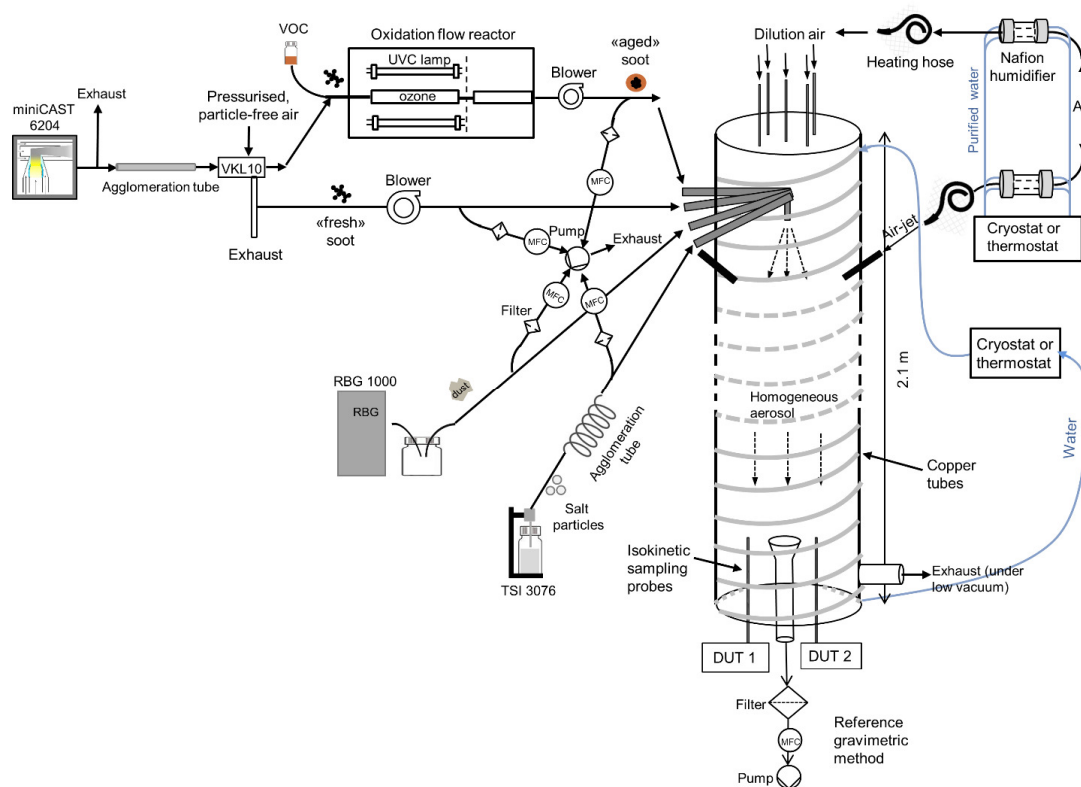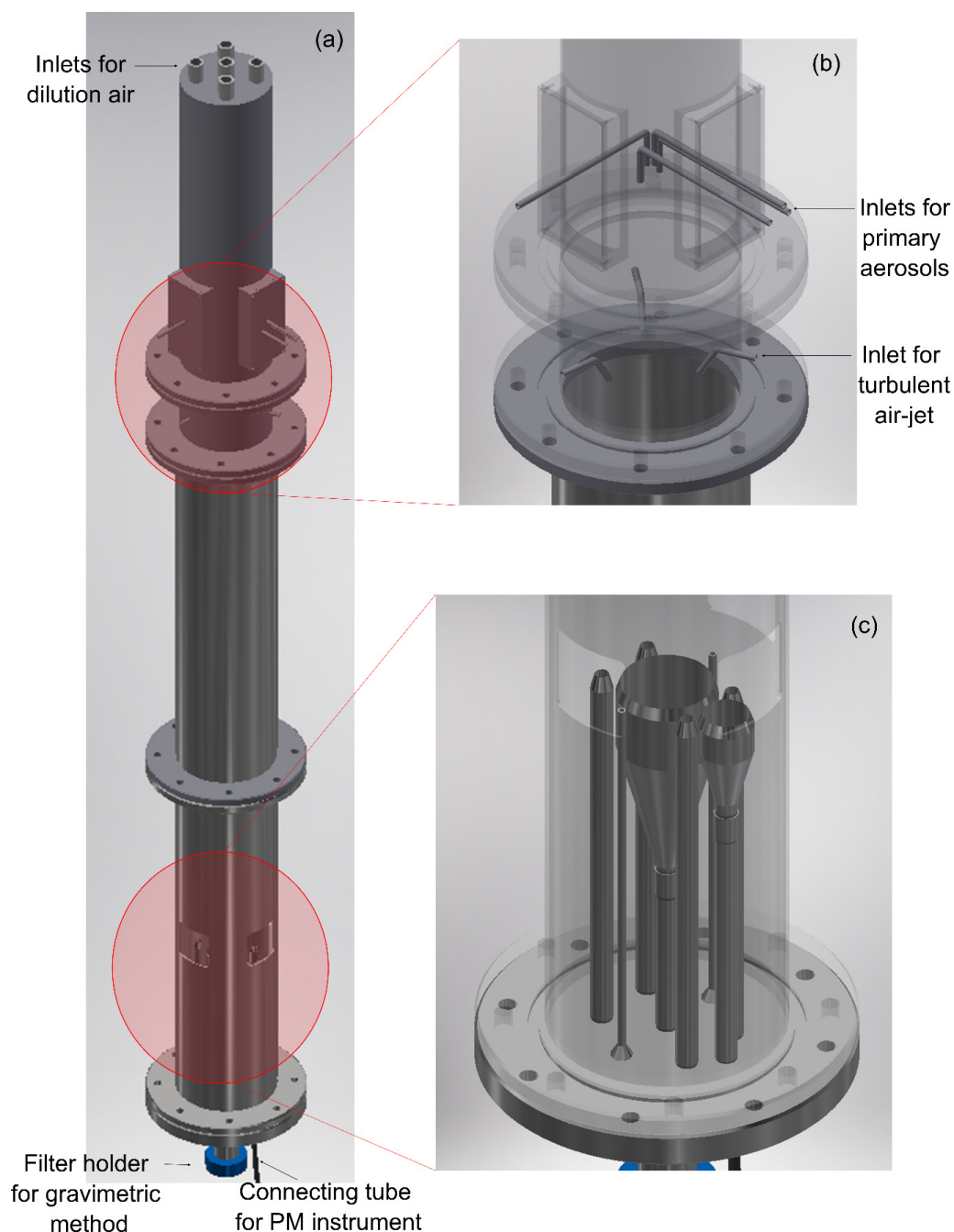639

640

641

642

643

644

645

Atmospheric
Measurement
Techniques
Open Access
EGU

Discussions

646

Figure 1: Schematic illustration of the experimental setup. DUT stands for device under test.

649   **Figure 2: a) Computer-aided design (CAD, Inventor Professional 2019, Autodesk, USA) of the homogeniser. Panels (b)**
650   **and (c) show enlarged views of the primary aerosol inlets and isokinetic sampling probes, respectively.**

Atmospheric
Measurement
Techniques
Discussions

Open Access

EGU
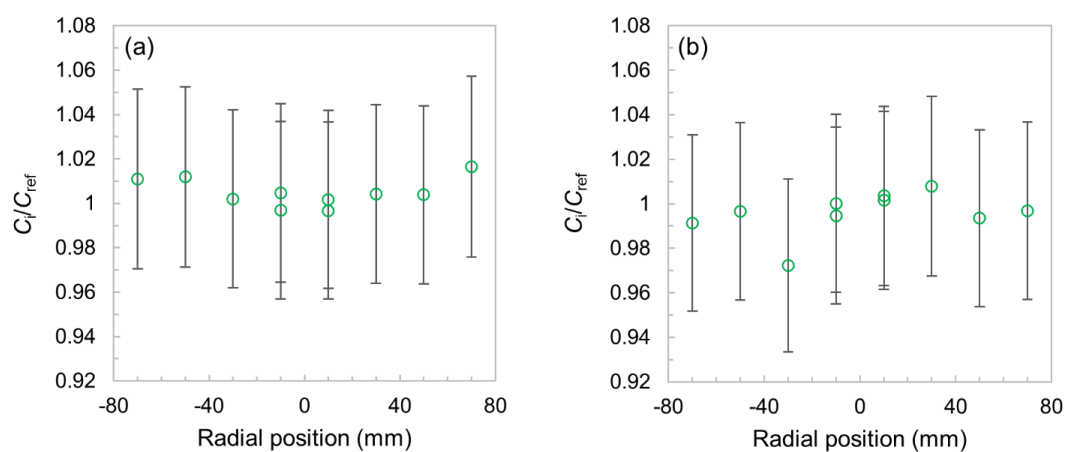
Figure 3: Aerosol spatial homogeneity, $\eta_{hom} = C_i/C_{ref}$, at various radial positions along the diameter of the flow tube with a) NaCl (sodium chloride) and b) mineral dust particles as test aerosols. The measurements at positions i = -10 mm and + 10 mm were performed twice to assess measurement reproducibility. The error bars designate expanded uncertainties (95 % confidence level). These are type B uncertainties from the combined measurement uncertainties of the two CPCs and have no influence on the determination of homogeneity since they would shift all data points up or downwards by the same amount.
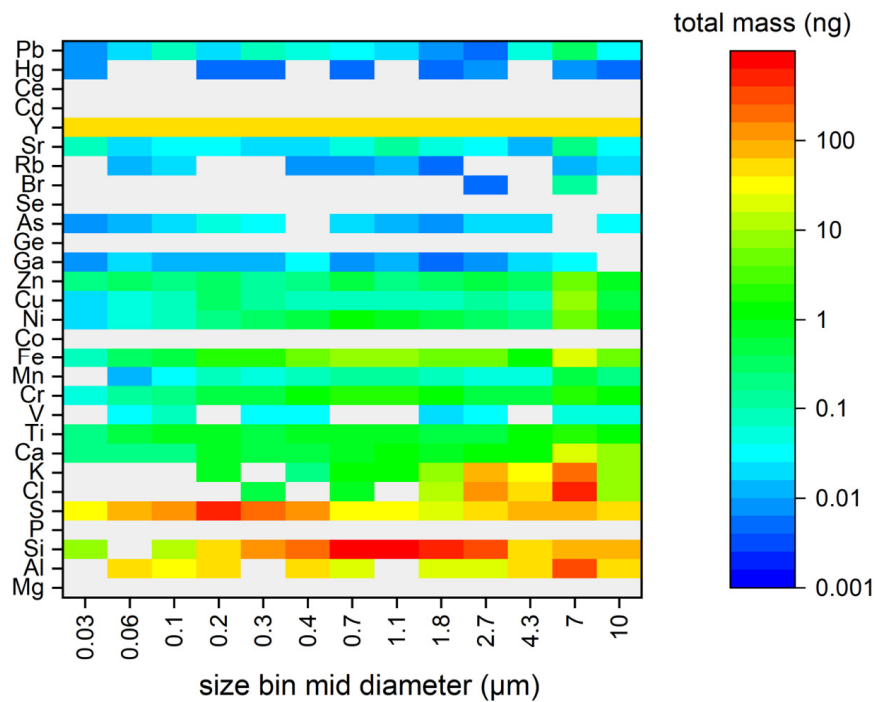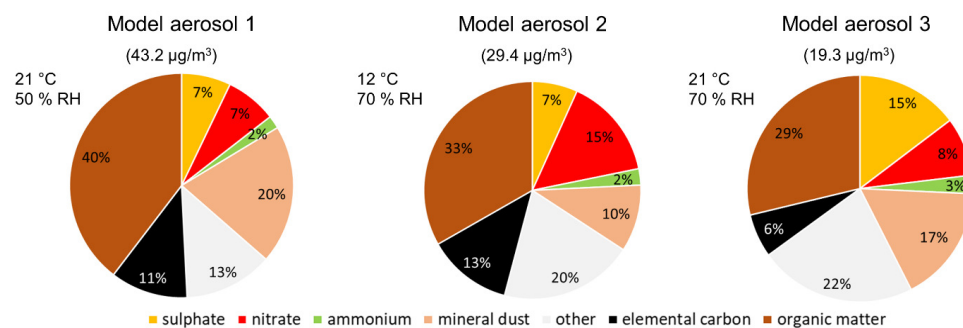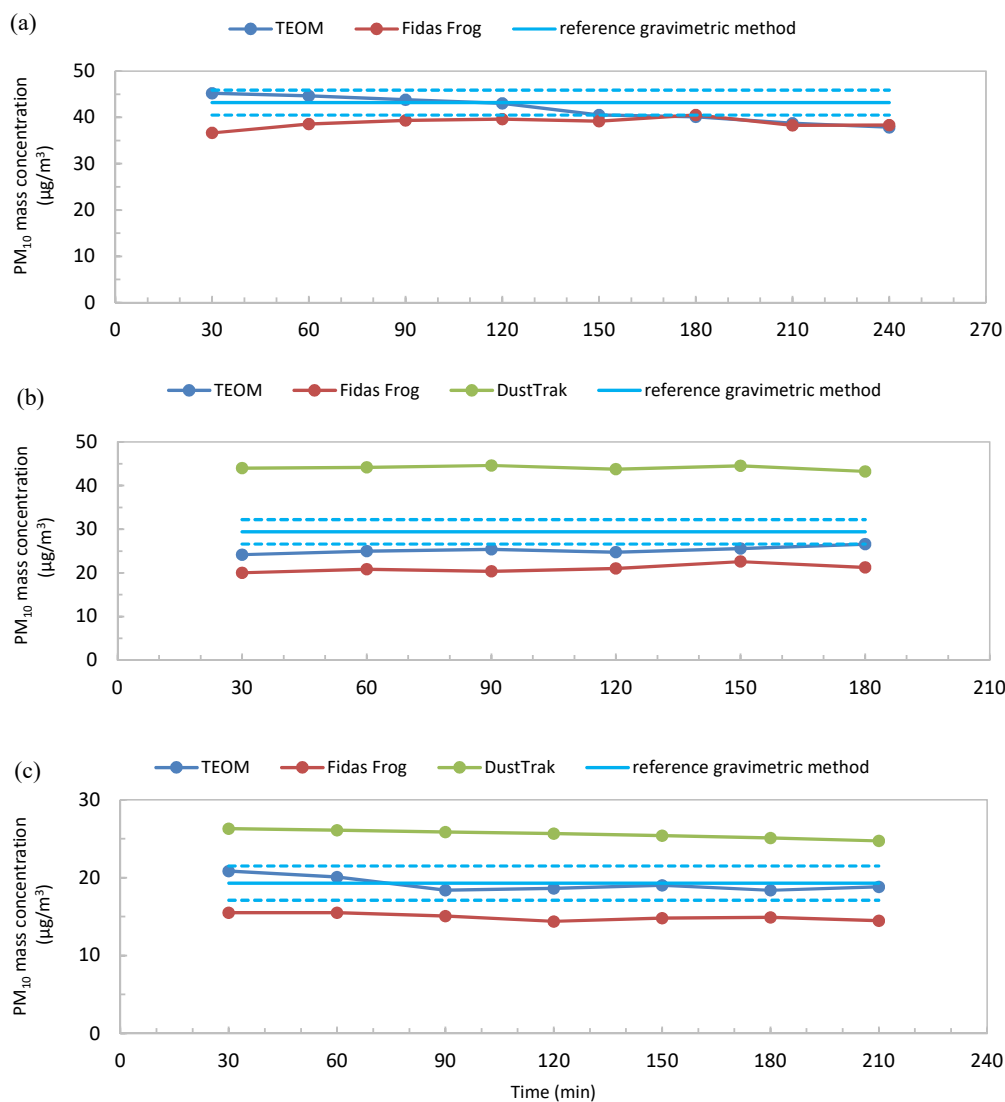
Figure 4: TXRF analysis of model aerosol 1 (see text and Table 2 for a discussion on all three model aerosols).

5 **Figure 5: PM composition (%) of the three model aerosols and environmental conditions during each experiment.**

Figure 6: PM$_{10}$ mass concentrations reported by the TEOM 1405, DustTrak DRX 8533 and Fidas Frog monitors compared to the results of the reference gravimetric method in the case of a) model aerosol 1, b) model aerosol 2 and c) model aerosol 3. In Fig. 6(a), the results of the DustTrak 8533 are not plotted because of technical issues during measurement (see text for more details). The dashed lines designate the expanded uncertainties (95% confidence level) of the reference PM$_{10}$ value.

23

15 **Table 1: Example of the uncertainty budget for a PM$_{10}$ mass concentration of 40 µg/m^3 and a sampling time of 240 min.**

Quantity	Value (example)	Standard uncertainty (k=1)	Relative uncertainty (95 % confidence level)
t	240 min	negligible	negligible
P_{rel}	1.00	0.01	2 %
η_{hom}	1.000	0.013	2.6 %
Q	38.333 L/min	0.058 L/min	0.30 %[1]
m	368.0[2] µg	8.4 µg	4.6 %
$C_{m,ref}$	40.00 µg/m^3	1.13 µg/m^3	5.7 %

[1] The mass flow meter (Natec Sensors GmbH, Germany) was calibrated at METAS in a traceable manner. The expanded relative uncertainty on the calibration certificate amounts to 0.15 %. Here, a conservative estimation of 0.30 % was made to
20 account for possible drifts since the time of calibration.

[2] Assuming no loss of particulate mass during filter conditioning.

25

30

35

Atmospheric
Measurement
Techniques
Discussions

Table 2: Chemical composition of the three model aerosols, mass concentration (µg/m³) of each chemical constituent and
40 **environmental conditions during each experiment.**

Model aerosol	Sulphate (µg/m³)	Nitrate (µg/m³)	Ammonium (µg/m³)	Mineral dust (µg/m³)	EC [1] (µg/m³)	OC [1] (µg/m³)	OM [2] (µg/m³)	Other [3] (µg/m³)	T (°C)	% RH
1	3.06 ± 0.13	3.17 ± 0.11	0.80 ± 0.12	8.6 ± 2.6	4.8 ± 0.6	10.0 ± 0.8	17.0 ± 3.4	5.5 ± 0.2	21 ± 1	50 ± 2
2	2.03 ± 0.09	4.53 ± 0.16	0.73 ± 0.20	3.0 ± 0.9	3.8 ± 0.5	6.0 ± 0.5	10.2 ± 2.0	6.0 ± 0.2	12 ± 1	70 ± 3
3	3.07 ± 0.12	1.75 ± 0.11	0.55 ± 0.10	3.5 ± 1.1	1.3 ± 0.2	3.6 ± 0.3	6.1 ± 1.2	4.7 ± 0.2	21 ± 1	70 ± 3

[1] The reported uncertainties do not include uncertainties in the determination of the split point.

[2] In past studies with atmospheric aerosols, factors between 1.1 and 2.1 have been proposed to convert OC to OM mass (El-
45 Zanan et al., 2005). The Micro Smog Chamber is known to yield moderately to strongly oxidised secondary organic matter
(Bruns et al., 2015), thus a factor of 1.7 ± 0.3 was assumed.

[3] Mostly Na^+ and to a lesser extent K^+ and Cl^- from contamination of the aerosol generation system and, possibly, impurities
in the mineral dust mixture.

50

55

60

Table 3: Average PM$_{10}$ mass concentration (μg/m^3) reported by the TEOM 1405, Fidas Frog and DustTrak 8533 automated PM
65 **monitors and the referene gravimetric method.**

	Average PM$_{10}$ mass concentration (μg/m^3)			
Model aerosol	TEOM 1405	Fidas Frog	DustTrak 8533	Reference gravimetric method
1	41.6	38.8	-[1]	43.2 ± 2.7
2	25.3	21.0	44.0	29.4 ± 2.8
3	19.2	15.0	25.6	19.3 ± 2.2

[1]The result was discarded because of a technical issue during measurement.